Research Square

Preprints are preliminary reports that have not undergone peer review.
They should not be considered conclusive, used to inform clinical practice,
or referenced by the media as validated information.

Global Vulnerability Assessment of Mobile Telecommunications Infrastructure to Climate Hazards using Crowdsourced Open Data

Edward Oughton

eoughton@gmu.edu

George Mason University https://orcid.org/0000-0002-2766-008X

Tom Russell

University of Oxford

Jeongjin Oh

World Bank

Sara Ballan

World Bank

Jim Hall

University of Oxford https://orcid.org/0000-0002-2024-9191

Article

Keywords:

Posted Date: April 4th, 2025

DOI: https://doi.org/10.21203/rs.3.rs-6190815/v1

License: This work is licensed under a Creative Commons Attribution 4.0 International License.
Read Full License

Additional Declarations: There is **NO** Competing Interest.

Version of Record: A version of this preprint was published at Nature Communications on August 3rd, 2026. See the published version at https://doi.org/10.1038/s41467-026-76197-w.

Global Vulnerability Assessment of Mobile Telecommunications Infrastructure to Climate Hazards using Crowdsourced Open Data

Edward J. Oughton[1*], Tom Russell[2], Jeongjin Oh[3], Sara Ballan[3], and Jim W. Hall[2]

[1]College of Science, George Mason University, Fairfax, VA, USA

[2]Environmental Change Institute, University of Oxford, Oxford, Oxfordshire, UK

[3]World Bank, Washington DC, USA

*Corresponding author: Edward J. Oughton (e-mail: eoughton@gmu.edu)

Address: College of Science, George Mason University, 4400 University Drive, Fairfax, VA

Abstract

The ongoing change in Earth`s climate is causing an increase in the frequency and severity of climate-related hazards, for example, from coastal flooding, riverine flooding, and tropical cyclones. There is currently an urgent need to quantify the potential impacts of these events on infrastructure and users, especially for hitherto neglected infrastructure sectors, such as telecommunications, particularly given increasing dependence on digital technologies. In this analysis a global assessment is undertaken, quantifying the number of mobile base stations potentially vulnerable to climate hazards using open crowdsourced data equating to 6 million 2G, 3G, 4G and 5G base stations. We find that for a 0.1% annual probability event under a high emissions scenario (RCP8.5), the number of potentially affected base stations is estimated at 1.61 million for tropical cyclones, equating to USD 1.62 billion in direct damage (an increase against the historical baseline of 20% and 11%, respectively). For coastal flooding the number of potentially affected mobile base stations for an event with a 0.1% annual probability under RCP8.5 is 92.2 thousand, equating to direct damage costs of USD 2.26 billion (an increase against the baseline of 75% and 85%, respectively). The findings demonstrate the need for risk analysts to include mobile communications (and telecommunications more broadly) in future critical national infrastructure assessments. Indeed, this paper contributes an assessment methodology and dataset for use in future research to assess this critical infrastructure sector using open data.

1. Introduction

Climate change is one of the major challenges of our time, with society and the economy needing to rapidly adapt to an increase in the frequency and severity of disasters (Pörtner et al., 2022; Simpson et al., 2021; Verschuur et al., 2024; Wuebbles et al., 2017). Adaptation of critical infrastructure is therefore essential, particularly for 'lifeline utilities', such as energy, transportation, water, waste, and telecom networks (Argyroudis et al., 2022; El-Bawab, 2021; Hoßfeld et al., 2023; Othman et al., 2023). However, infrastructure assessment research focusing on climate vulnerability has largely neglected telecommunication infrastructure, defined here as consisting of 2G, 3G, 4G and 5G base stations, local fixed broadband networks, long-distance land and submarine fiber networks, satellite networks, and cloud data centers.

For example, whereas there have been evaluations for other critical infrastructure sectors such as transportation (Gössling et al., 2023; Koks et al., 2019; Verschuur et al., 2023) or power (van Vliet et al., 2016), the global vulnerability assessment of telecommunication infrastructure from natural disasters has received little systematic consideration in the literature. Very often there has been a focus on field-based post-disaster damage evaluation, after flooding or tropical cyclones. Examples of telecommunication infrastructure damage assessments for natural disasters between 2005-2011 include the Katrina, Gustav and Ike hurricanes, Chile's 2011 earthquake and tsunami, New Zealand's 2011 earthquake in Christchurch, and the Great Earthquake and Tsunami in the Tohoku Region of Japan (Krishnamurthy et al., 2016; Kwasinski, 2011). Unfortunately, more recent critical infrastructure cost-benefit assessments have focused on strengthening infrastructure assets, yet have excluded telecommunication infrastructure (Hallegatte et al., 2019). This is also surprising because communicating via telecommunication infrastructure plays a vital role in natural hazard preparedness and resilience, both through early warning and recovery (Coughlan de Perez et al., 2022; Hermans et al., 2022; Marshall et al., 2023).

The contribution of this analysis is to begin to fill this literature gap by developing new methods to evaluate the climate hazard vulnerability of mobile cellular infrastructure assets. This is important because quantitative scenario analysis can produce geospatial hazard information that can be used in multiple different ways. Firstly, such information can help support adaptation decisions by policy makers and/or Mobile Network Operators, with regards to strengthening existing infrastructure assets (Hall et al., 2017). Secondly, such information can inform location planning of future assets, along with building design codes for extra protection in areas of higher vulnerability from multi-hazard threats (Pourghasemi et al., 2020; Yousefi et al., 2020). Finally, hazard information can enable risk exposure to be shared among many different parties, for example, by businesses and households sharing risk with insurers (who in turn share risk with re-insurers) (Broberg, 2020; Dallimer et al., 2020). To move towards these adaptation options, it is imperative that a strong vulnerability assessment method is

identified, particularly as such an approach can support the inclusion of this sector in future cross-sectoral appraisals.

Given the issues raised in this introduction, the following research questions guide the climate vulnerability assessment of mobile cellular infrastructure:

I. How many cellular assets are potentially vulnerable to climate hazards, here comprising coastal flooding, riverine flooding, and tropical cyclones?
II. What magnitude of direct economic damage may occur from different climate hazard scenarios, for example from flooding, riverine flooding, and tropical cyclones?

In the following section (Section 2) a literature review is presented to explore the range of related studies assessing climate hazard impacts on telecommunications infrastructure. Next, a method is detailed in Section 3 to obtain the necessary results to answer the research questions articulated. Subsequently, Section 4 reports results obtained, before a discussion of the key findings is undertaken in Section 5. Finally, conclusions are given in Section 6.

2. Literature review

The telecommunications sector consists of a wide range of infrastructure assets, including cellular towers, copper and fiber optic cables, switches, satellites, Wi-Fi and small cell hotspots, and long-range microwave radio links (Hall et al., 2016; Oughton et al., 2018; Pant et al., 2020). There are challenges to obtaining data on many of these assets as they are very often built by private companies (and thus commercially sensitive), as well as being hard to identify from other methods (e.g., aerial or satellite imagery) (Brewer et al., 2021; Mohebbi et al., 2020; Oughton and Mathur, 2021). Such data limitations have often constrained analysis on this sector, leaving many assessments focused on small case study areas.

Disrupted mobile communications in disaster zones leads to poor coordination and decision making, as disaster response professionals and resources are not directed to areas most in need (EL Khaled and Mcheick, 2019; Kaja et al., 2021). Moreover, when emergency organizations are unable to effectively coordinate and communicate, this can also lead to catastrophic outcomes for both human life and properties, particularly as threats from hazard environments evolve over time during disaster events (Rosario-Albert and Takahashi, 2021). Given the convenience of owning a cell phone, when a disaster does take place, this is often the only communication device available for first responders and for citizens attempting to contact others (Foster, 2011). Therefore, telecommunication sites need to be provisioned to provide resilient service in such circumstances, with decision-makers selecting the most optimal network architecture and design specifications to ensure reliable service (Gallarno et al., 2023).

There are only a very limited number of post-event damage assessments of telecommunication networks in the literature, evaluating the extent to which water and wind damage interrupt telecommunication assets, and the voice and data services they provide (Kwasinski, 2013; O'Reilly et al., 2006). Often these have been carried out for major hurricanes when evaluating impacts to a range of critical infrastructure sectors including power networks. Following Hurricane Katrina, on-site surveys of damage were conducted to observe the impacts on broadband networks, with substantial disruption taking place to centralized network elements (not just distributed network assets) (Kwasinski et al., 2009). Overall, Hurricane Katrina is estimated to have led to the failure of more than 1,000 cellular sites, although 80% were able to be put back online within one week (as base station realignment and restoring power was often sufficient), whereas the 20% more severely damaged were in Gulf coast areas more severely affected (and thus required more substantial repairs or full replacement) (Federal Communications Commission, 2006). This contrasts with 320 cell site failures during Hurricane Harvey, equating to approximately 4.1% of the 7,804 cell sites in coastal counties exposed in Texas and Louisiana (Federal Communications Commission, 2017).

Generally, two main failure effects can occur. Firstly, the impact of flooding leads to direct floodwater contact to active electronic components, including backup generators, fuel tanks, as well as network equipment, leading to disruption. During Hurricane Katrina, while the elevated mounting of some cellular assets helped reduce recovery time by avoiding flood damage in the New Orleans area, many cellular sites had inconsistent cell site construction practices. Indeed, often only part of the base station equipment present may be elevated above the flood plain, and therefore protected from floodwaters, leaving some telecom components or necessary energy equipment vulnerable. Secondly, logistical issues can cause fuel required for maintaining backup generators to never reach key assets, leading to a loss of power (Kwon et al., 2016). When this damage does occur, rebuilding costs can be very high. Following damage caused by Hurricane Matthew in The Bahamas, telecommunications constituted up to 63% of the total cost for replacing damaged infrastructure assets across the archipelago, as many sites had been flooded and affected by wind damage (Bello et al., 2020).

The impact on cellular telecommunications infrastructure from natural hazards has been characterized by five potential damage states (Kwasinski, 2011), which include:

I. The absence of permanent onsite backup electricity generation equipment, combined with exhausted onsite backup battery packs, leading to loss of service.
II. Failure of permanent onsite backup electricity generation equipment leading to loss of service. This outcome could occur through usage of all backup fuel and poor maintenance of generation equipment leading to a failure to start.

III. Substantial damage to onsite backup electricity generation equipment while leaving communications equipment (e.g., active radio equipment) fully functioning. Frequently onsite backup electricity generation equipment may be placed at ground level, even if active radio electronic equipment is elevated to avoid floodwater damage.

IV. Severe loss of functionality to both active electronic radio equipment and onsite backup electricity generation equipment.

V. Catastrophic damage, leading to failure, in other infrastructure assets necessary to provide normal service. For example, this could be physical damage to fiber optic backhaul cables or other ground-based switching equipment, or misalignment of wireless backhaul units leading to interrupted or severely degraded services.

Hazards also pose a major risk to the civil engineering structures used to mount radio antennas. Indeed, the actual tower design can have a large impact on how affected an asset may be, with three main designs including monopoles, self-supported structures, or guyed structures. Often monopoles extend up to 60 meters and consist of hollow cantilevered structures and are commonly used in urban areas where land costs are prohibitively high for other designs. For greater height, lattice structures are used to provide self-supported towers up to 120 meters. Finally, for heights up to 500 meters, guyed structures consist of a modest narrow mast with lateral stability, supported by multiple ground anchors via tensioned guy cables (Suryakumar et al., 2020). In rural areas where land costs are lower, it is more common to utilize higher guyed structures.

Cell phone towers have typically been built to withstand certain hazard exposures (e.g., wind speeds) above which they may fail. However, they are still vulnerable and at risk from hazards below these thresholds too, for example, via high wind speeds during hurricanes. Throughout Hurricane Maria in 2018, winds of up to 280 km/h felled more than 90 percent of the cell phone towers in Puerto Rico. Risks are more moderate at lower wind speeds, with ~25% of towers downed by ~80mph winds in New York during Hurricane Sandy (Woetzel et al., 2020). Additional information can be found in a report published by the Public Safety and Homeland Security/ Bureau Federal Communications Commission (2018) which provides data about the impact of hurricane Harvey, Irma, Maria, and Nate on communication infrastructures.

Aside from physical damage, unaffected cellular network assets can also be overloaded following a disaster due to heavy traffic congestion, preventing the proper functioning of mobile voice and data services. Empirical evidence from wireless network operators demonstrates how wireless traffic sees a statistically measurable increase during extreme events (Jakubek, 2015), often exceeding the load each asset was provisioned for at the design stage, potentially leading to interrupted or severely degraded service.

Cellular network planning traditionally does not place much emphasis on potential natural disaster scenarios. A standard planning approach consists of three stages (Oughton et al., 2022a) where a network operator first undertakes high-level regional assessment of new asset deployments. Secondly, cluster-level evaluation is undertaken for a set of cells within a defined geographic proximity (e.g., 20 km²). Finally, high-fidelity link-level radio simulations are utilized to optimize cell site location, antenna designs, power levels, tower heights, pathloss, predicted interference and link margins. The aim is to maximize coverage and capacity, while minimizing the cost of any necessary investment. As new spatial patterns of traffic demand emerge, the network operator iteratively redesigns the system of cells, by partitioning existing coverage areas and building new assets (Eiselt and Marianov, 2012). Due to cost considerations, moving existing major cell sites is generally avoided.

In terms of risk assessment, there has only been very limited research published focusing on deductive appraisals of future risks. One example utilizes event-based storylines to evaluate the impact of future climatic and socioeconomic conditions for critical infrastructure in coastal flood areas (Koks et al., 2022). A lack of data has held back evaluation. Critical infrastructure asset locations have been derived from OpenStreetMap, consisting of only 141,478 communication towers and 80,750 masts globally (Nirandjan et al., 2022). This is only a tiny fraction of global sites, providing motivation for the use of more expansive crowdsourced methods.

This literature review identified (i) why mobile telecommunication infrastructure plays such an important role during disaster events, (ii) the different types of damage states that might occur to mobile assets, and finally (iii) identified some of the more recent deductive evaluations of this critical infrastructure sector. In the light of this previous research, a method capable of answering the research questions will be outlined.

3. Method

The geospatial assessment method (Figure 1) consists of multiple steps, including the selection of scenario parameters, global hazard models and affiliated data, and then intersection processing of geolocated mobile base stations to undertake a vulnerability assessment using exposure-damage curves to produce the required results. The method steps will now be articulated in detail.

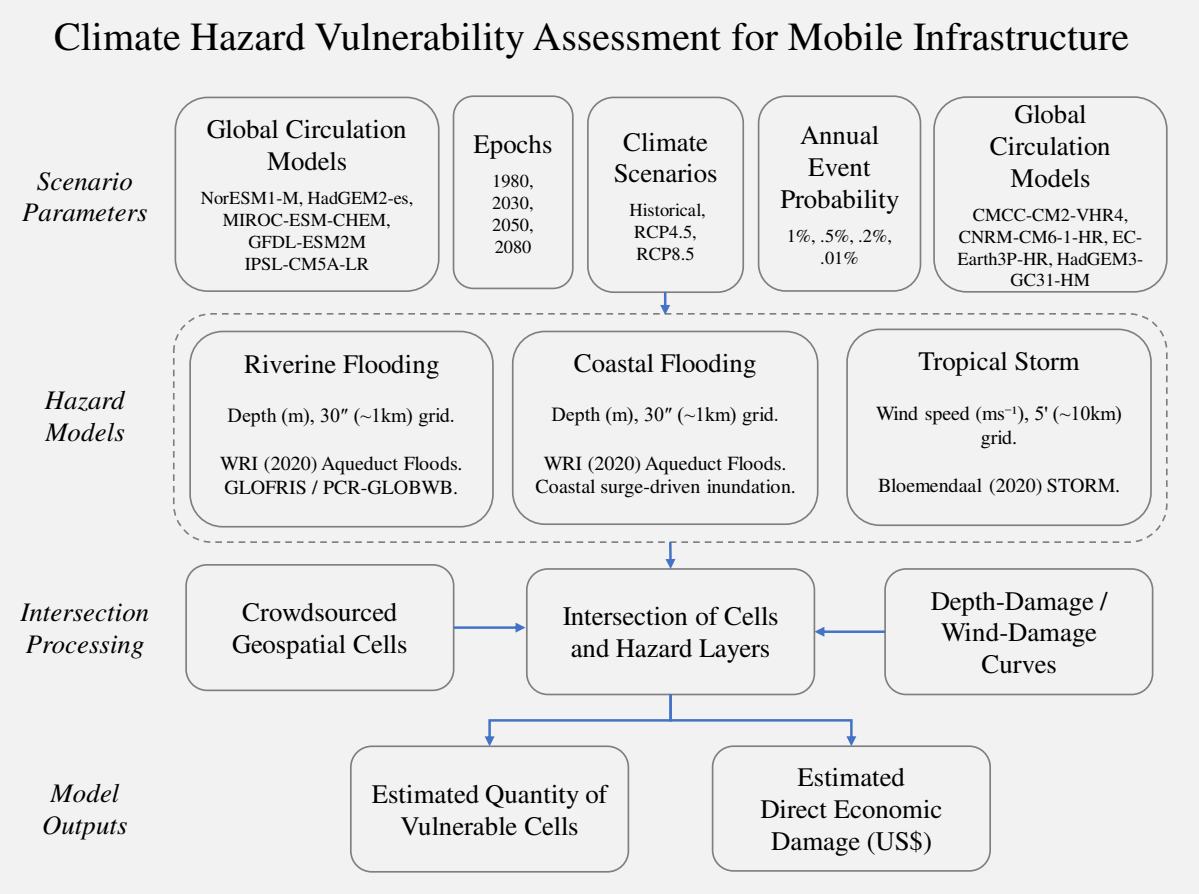


Figure 1 Overview of modeling method

3.1. Climate hazard data

For river and coastal flooding, the Global Aqueduct geospatial hazard datasets (World Resources Institute, 2022) are available for two climate scenarios (as well as a 1980 historical baseline), from the CMIP5 (Coupled Model Intercomparison Project Phase 5) archive. These include (i) Representative Concentration Pathway 4.5 (steady carbon emissions) (intermediate climate outcomes) (RCP 4.5) and (ii) Representative Concentration Pathway 8.5 (rising carbon emissions) (limited climate outcomes) (RCP 8.5).

The former scenario (RCP 4.5) is seen to be a mid-range, reflecting considerable carbon mitigation by 2040 onwards. Whereas the latter (RCP 8.5) models rising carbon emissions with little carbon mitigation taking place (thus, Earth's current global trajectory is closest to RCP 8.5). Four main return periods are also selected for assessment, including events equating to 1% annual probability (1-in-100-year), 0.4% annual probability (1-in-250-year), 0.2% annual probability (1-in-500-year), and the most extreme 0.01% annual probability (1-in-1000-year).

In this analysis, coastal hazards represent storm surge flooding along coastlines with simulation projections from sea level change derived from the RISES-AM project. Three different sea rise scenarios are selected based on the 5th, 50th and 95th RISES-AM percentiles. Additionally, scenario layers which include estimated subsistence impacts are included in the analysis.

Riverine hazards in this evaluation represent overflow river flooding events, most likely to occur in river basins from excessive water loads. The Aqueduct river hazard modelling used the PCRaster Global Water Balance hydrological model to simulate flood inundation, with forcing data for future climate conditions taken from the Inter-sectoral Impact Model Intercomparison Project (ISI-MIP) (Hempel et al. 2013). This provides hazard maps for each of five global circulation models (GCMs) from different institutions: (i) GFDL-ESM2M from the US Geophysical Fluid Dynamics Laboratory (NOAA), (ii) HadGEM2-es from the UK Met Office Hadley Centre, (iii) IPSL-CM5A-LR from the French Pierre-Simon Laplace Institute, (iv) MIROC-ESM-CHEM from the Japanese Atmosphere and Ocean Research Institute (The University of Tokyo), National Institute for Environmental Studies, and Japan Agency for Marine-Earth Science and Technology, and (v) NorESM1-M from the Bjerknes Centre for Climate Research, at the Norwegian Meteorological Institute. This analysis does not aim to preference a specific model, instead opting to use these capabilities as an ensemble to obtain broad statistical estimates given each of these five global circulation model options.

Figure 2 illustrate the sum of flooded pixels by continent and flood region, respectively, by annual probability, year, and climate scenario. The mean average is taken across the different riverine models.

Figure 2 subplot (A) illustrates large increases in coastal flooding over the different climate scenarios, with a clear upward trend in higher emissions environments. In comparison, riverine flooding sees a more mixed result, with either only minor increases in flooded area (e.g., North America or Sub-Saharan Africa), or a static trend (e.g., Western Europe). The literature has already identified highly heterogenous riverine flooding impacts (especially for Europe) (Blöschl et al., 2019), with high variability between flooding models leading to greater uncertainty in flooding impacts (especially for high emissions scenarios) (Bernhofen et al., 2018).

Return period maps for maximum wind speeds experienced during tropical cyclones are obtained from Bloemendaal et al 2020 and 2022 for present and future (2050s, SSP5-8.5) climate conditions, for a fixed set of return periods between 10 and 10,000 years, at 10 km resolution, for each cyclone basin (Bloemendaal et al., 2022, 2020). The future climate conditions are derived from a set of general circulation models: CMCC-CM2-VHR4, CNRM-CM6-1-HR, EC-Earth3P-HR and HadGEM3-GC31-HM. These models are evaluated and briefly described in the literature (Roberts et al., 2020). Each set of return period maps is calculated from 10,000 years of synthetic tracks modeled using the Synthetic

Tropical cyclOne geneRation Model (STORM). The global maximum windspeed return period maps are mosaiced together across all basins to provide global GeoTIFFs (Russell, 2022).

3.2. Mobile infrastructure asset data

Crowdsourced data for December 2022 are gathered from OpenCelliD for current mobile infrastructure networks, covering 6 million 2G, 3G, 4G and 5G base stations. The Global System for Mobile Communications (GSM) is regarded more commonly as the second cellular generation or '2G'. following standardization in 1991, commercial deployments were launched across the world in the 1990s onwards, with the technology offering revolutionary voice and text Short Messaging System (SMS) services. A total of 10.3% of the base stations in the dataset as 2G, equating to a total of 0.78 million. Although outdated in many high-income countries, 2G is still very much widely used technology, especially in low- and middle-income countries.

The third cellular generation known as '3G' consists of multiple technologies, with the main standard known as the Universal Mobile Telecommunications System (UMTS). Standardized in 2001, commercial launches widely took place throughout the 2000s. The key benefit of 3G deployment was the introduction of basic data capabilities, enabling users to access a peak connection speed of ~3 Mbps. This enables web browsing and very basic low-resolution video functions. Approximately 41.9% of the assets in the dataset are 3G, equating to 3.18 million base stations.

The fourth generation of cellular technology ('4G') was standardized in 2009 with the name Long Term Evolution (LTE) and brought mass market mobile broadband to billions of consumers around the world (mainly deployed in the 2010s onwards). This was driven by the introduction of smartphones as a key general-purpose technology, largely resulting from Apple's pioneering iPhone. With peak speeds capable of up to ~100 Mbps, users have the capability to download high-definition video while mobile, as well as carry out a large range of online activities, most notably sharing and consuming high-quality content across a range of social media platforms. The dataset contains 3.63 million 4G LTE assets, comprising roughly 47.8%.

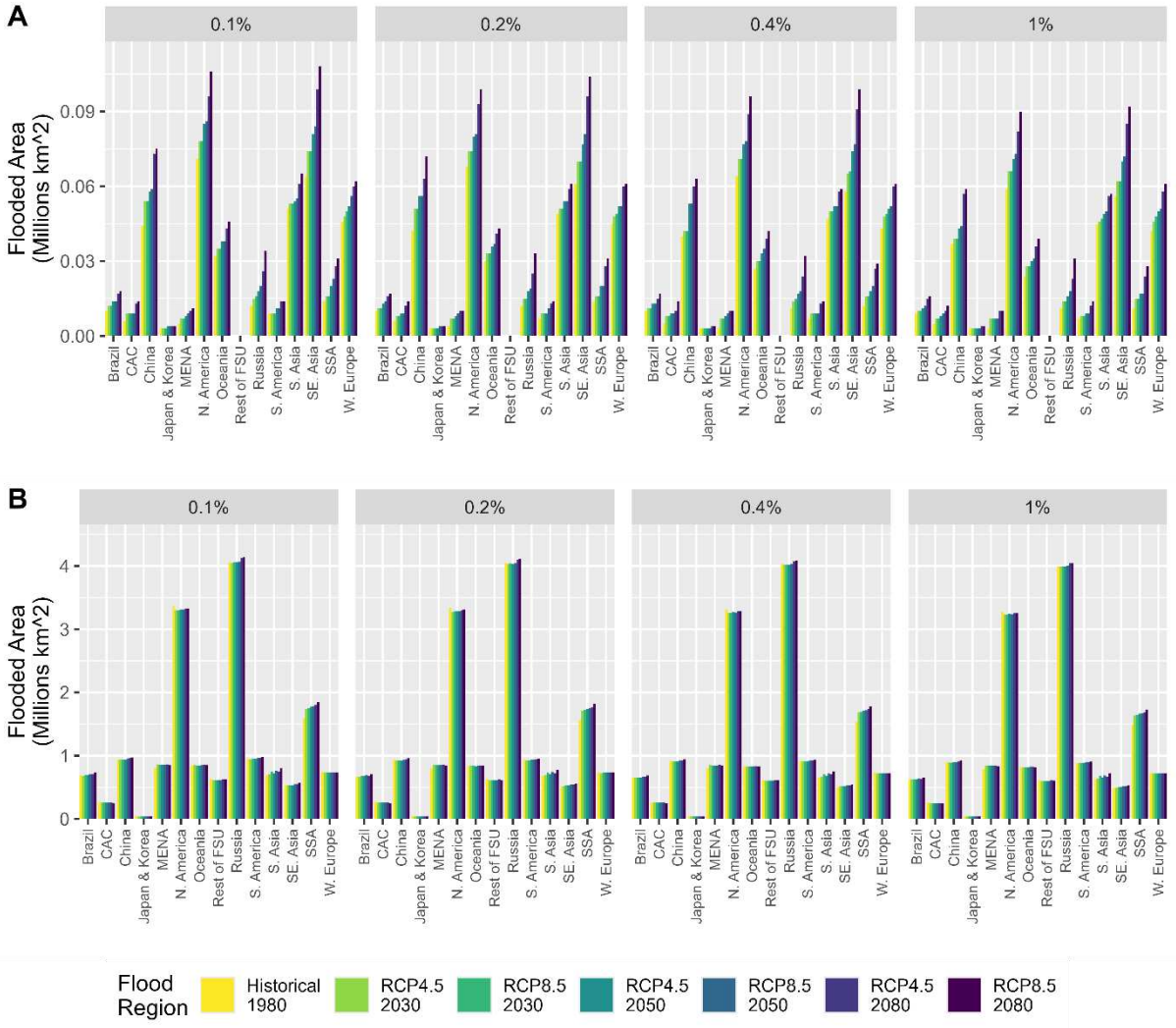


Figure 2 (A) Global sum of flooded coastal area by scenario, continent, annual probability and climate scenario, (B) Global sum of flooded riverine area by scenario, continent, annual probability and climate scenario.

Finally, the introduction of the fifth generation of cellular technology known as 5G has only fully taken place in recent years, from approximately 2020 onwards (Oughton et al., 2021). The standardized radio technology is referred to as the 5G New Radio (NR) standard (Cave, 2018; da Ponte et al., 2023; Lehr et al., 2021). Three key use cases exist for users, including enhanced mobile broadband, ultra-reliable low-latency communications, and massive machine type communications (Bauer and Bohlin, 2022; Oughton and Lehr, 2022). Given the limited number of countries with commercial 5G launches, less than 0.04% of the sample consists of 5G NR base stations (<2,718 assets). However, over the next decade, older base stations will be decommissioned and replaced with 5G NR equipment. Therefore, this number is expected to significantly increase in coming years, especially as higher-income countries turn off older generations such as 2G GSM.

3.3. Vulnerability analysis

Mobile cellular towers generally consist of the three main design types identified within the literature review, including monopoles, self-supported structures, or guyed structures. These assets usually rely on steel or aluminum for the structural frame, utilizing concrete at the base of the tower either for the foundation plinth or to secure guy lines. Vulnerability to hazards and the consequential damage cost is estimated using a damage curve approach, which is a standard way in the literature to relate, for example, the depth of flooding inundation or wind speed to a potential direct damage cost (DHS and FEMA, 2011; Miyamoto International and World Bank, 2019; Movahednia et al., 2022; Sánchez-Muñoz et al., 2020). However, there are not readily available damage curves for communication towers. Therefore, existing studies in the literature adopt a similar approach to assessing the vulnerability of electricity infrastructure assets, such as distribution poles and transmission pylons which share similar structural characteristics (Kok et al., 2005). Indeed, some studies utilize curves from the US HAZUS model (DHS and FEMA, 2011) for electricity infrastructure, to assess the vulnerability of communications infrastructure assets (Koks et al., 2022), as will be adopted here. Unfortunately, within the US HAZUS model, the development of fragility relationships specifically for telecommunications infrastructure assets based on inundation has been stated as "deferred to a later date" (p7-10), with no current update on the status of these improvements (DHS and FEMA, 2011) (thus, identifying an important area of future research).

Booker et al (2010) define fragility curves for each failure mode of cellular sites due to wind speed. These fragility curves are at the level of individual failure modes (e.g., foundation failure) rather than at the level of a complete cellular tower site because different failure modes have various implications for the functionality of the cellular site. For example, loss of cellular antenna at a given tower would prevent that tower from receiving or broadcasting calls, but it would still be able to relay calls from other towers if its microwave dish or fiber–optic link was functional. However, if the tower experiences structural failures, it would not be able to service incoming calls, outgoing calls, or relay calls through its microwave dish, but it would still be able to serve as a relay through its fiber–optic cable if the necessary power supply and supporting equipment were functional (Booker et al., 2010).

The investment costs for rebuilding mobile assets are adapted from the existing literature (Oughton et al., 2022b), to enable damage costs for different sized events and climate scenarios to be estimated. Broadly, the cost of building a new three-sector 4G macro cell site is approximately $100,000, equating to approximately $33,333 total capital expenditure per base station. Thus, a cell with a flooding depth of 0.6 meters and a damage quantity of 0.5, leads to a direct damage cost estimate of $16,666.5. As identified in the literature review, the specifics of the damage depend on the cell tower construction. At the lower end of the fragility curve, damage to electronic equipment could take place. Whereas in more

severe outcomes, this could include the full destruction of both active electronic radio equipment and passive civil engineering tower structures, requiring a total rebuild of a site.

The intersection process is carried out practically using a range of python packages. For example, managing spatial point data is carried out via *geopandas*, and then raster-based queries of the hazard layers are undertaken using a combination of *rasterio* and *rasterstats*. For each lower layer region, this information is exported to a comma-separated value file, and then later aggregated for reference in the following results section.

4. Results

The results will now be reported for coastal flooding, riverine flooding, and tropical cyclone hazards. First a set of metrics is presented which summarizes the main hazard differences per scenario. Next, the estimated results for mobile broadband infrastructure vulnerability are presented for each threat.

4.1. Vulnerability to coastal flooding

The number of vulnerable base stations at risk from coastal flooding is reported in Figure 3 (A) by year, and annual probability for various climate scenarios. For coastal flooding events with a 1% annual probability, equating to a 1-in-100-year event magnitude, 42.5 thousand assets are at risk when considering the historical 1980 climate scenario. However, by 2080 the number of vulnerable assets is estimated to increase to 67.7 thousand in the RCP4.5 scenario, and 74.4 thousand in the RCP8.5 scenario (an increase of 59% and 75%, respectively). In contrast, a 1-in-1000-year event with a 0.1% annual probability is estimated to affect 52.6 thousand annual base stations in the 1980 historical climate baseline. In the RCP4.5 scenario by 2080, this leads to an estimated increase to 82 thousand vulnerable base stations (a 56% increase), with up to 92.2 thousand base stations vulnerable in the RCP8.5 climate scenario (a 75% increase).

In Figure 3 (B), the analytical results are presented for the direct economic damage caused to assets from coastal flooding. The historical baseline for an event with a 1% annual probability (a 1-in-100-year event) is estimated at $0.95 billion, with this figure increasing to $1.56 billion by 2080 in the RCP4.5 scenario, and $1.76 billion in the RCP8.5 scenario (an increase of 64% and 85%, respectively). For larger events, such as those with a 0.1% annual probability (a 1-in-1000-year event) the historical baseline estimates a $1.22 billion impact, with this rising by 2080 to $2 billion in the RCP4.5 scenario (an increase of 64%), and $2.26 billion in the RCP8.5 scenario (an increase of 85%).

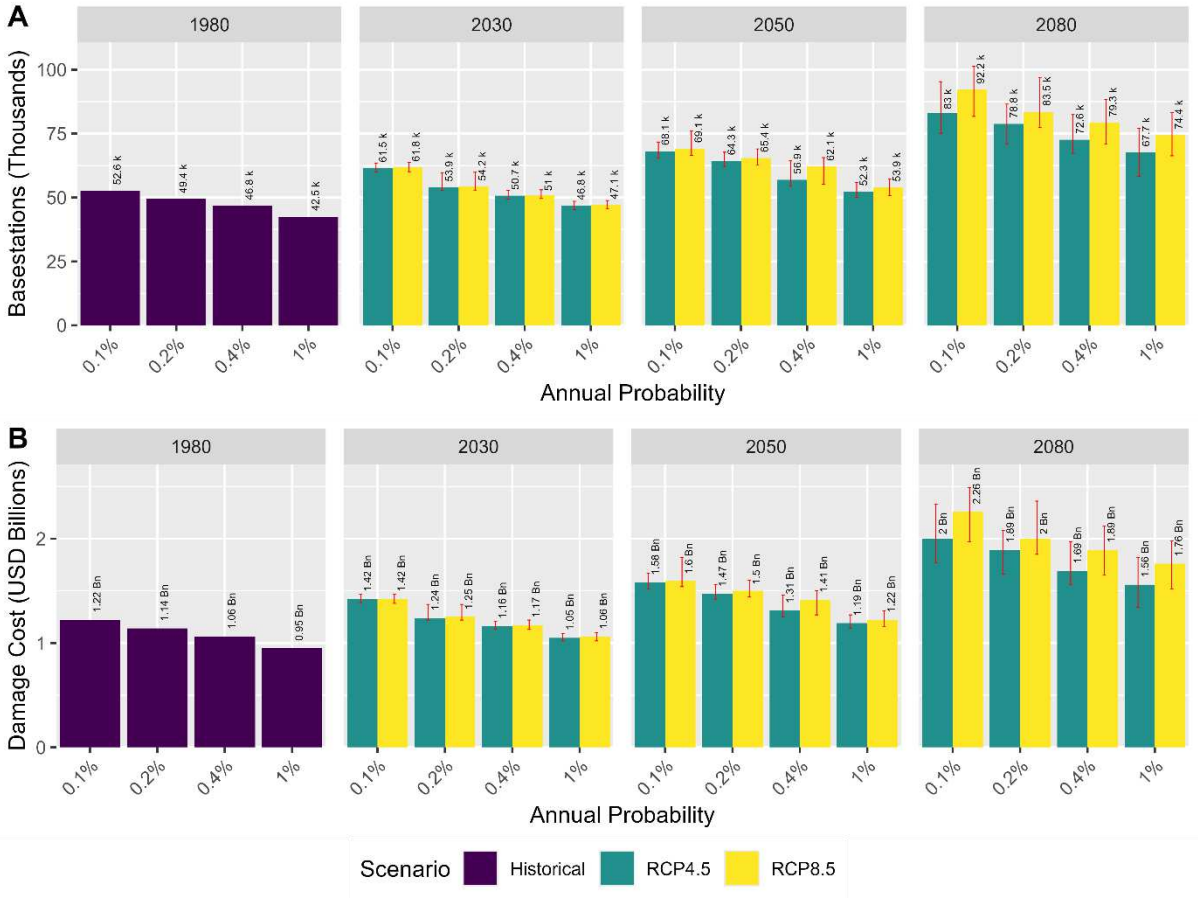


Figure 3 (A) Estimated coastal flooding impact to mobile voice/data basestations, reported by annual probability, year and climate scenario, (B) Estimated coastal flooding direct cost, reported by annual probability, year and climate scenario.

To provide greater geospatial insight, Figure 4 illustrates the estimated coastal flooding impacts for the RISES-AM model, with subplot (A) illustrating the cost density (adjusting for statistical area size), and subplot (B) visualizing the total cost per statistical area. For the RCP8.5 scenario in 2080, an event with a 0.01% annual probability (1-in-1000-year), large impacts are visible in Western Europe (e.g., The Netherlands, Germany, France, UK, Denmark), East Asia (e.g., China and Japan), Southeast Asia (e.g., Indonesia and Malaysia), North America (e.g., USA and Canada), and Latin America (e.g., Brazil, Mexico). The highest quantity of estimated vulnerable base stations and affiliated damages are in Asia (55 thousand equating to 60%), Europe (27 thousand equating to 31%), and North America (7 thousand equating to 8%).

As the underlying crowd-sourced data contains more users and thus more asset data for higher income countries, the results see the largest impacts overall in this income group. For example, across the scenarios approximately 53% of the vulnerable base stations assessed for coastal flooding are in high income countries, compared to an estimated 37% upper middle-income countries, and 10% in lower

middle-income countries. The lack of base station data available for low-income countries leads to very low estimated impacts for this income group (<1%).

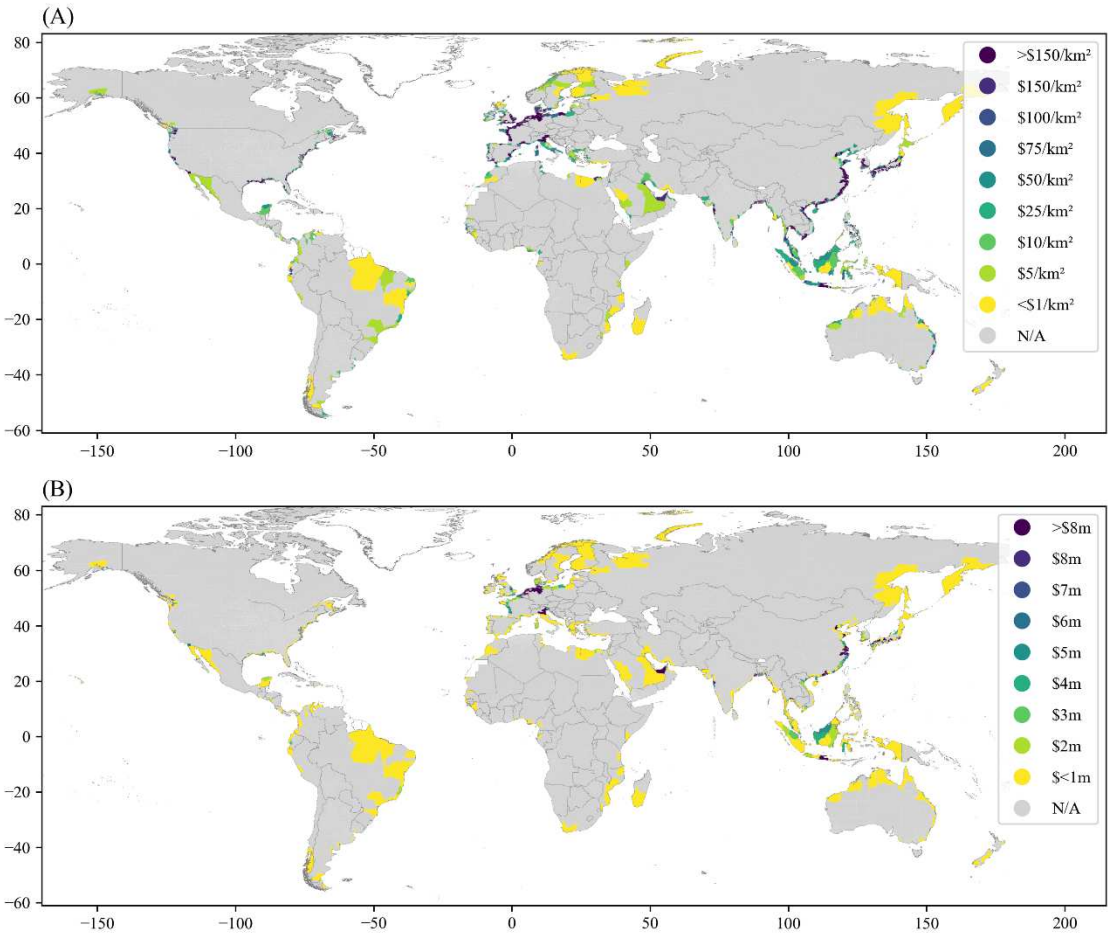


Figure 4 (A) Cost density of estimated coastal flooding direct damage ($/km^2), (B) Total cost of estimated coastal flooding direct damage ($ millions).

4.2. Vulnerability to riverine flooding

Next, Figure 5 (A) reports the number of base stations vulnerable to riverine flooding. For this hazard there is less of a pronounced trend between more severe climate scenarios and increasing cellular asset vulnerability. For example, the historical baseline from 1980 estimates a total number of vulnerable base stations to be 0.79 million for events with a 1% annual probability (a 1-in-100-year return period), up to 0.84 million for events with a 0.1% annual probability (a 1-in-1000-year return period). Thus, vulnerability estimates are estimated to see mixed impacts over time. Approximately, 0.79 million base stations at risk in 2080 in the RCP4.5 scenario, and 0.8 million base stations at risk in 2080 in the RCP8.5 scenario (a 1% increase), for events with 1% annual probability. Similar results occur for the 1-in-1000-year return period, equating to 0.1% annual probability, with 0.84 million base stations at risk in 2080 in the RCP4.5 scenario, and 0.85 million base stations at risk in 2080 in the RCP8.5 scenario.

Therefore, in Figure 5 (B) the direct economic damages follow this decreasing trend. For example, in the less severe case of events with a 1% annual probability (a 1-in-100-year return period), the estimated damage ranges from $11.3 billion in the historical 1980 baseline to 2080 estimates of $11.3 billion in the RCP4.5 climate scenario (essentially no change), and $11.7 billion in the RCP8.5 climate scenario (a 4% increase). In the more severe event case of 0.1% annual probability (a 1-in-1000-year return period), the estimated damage ranges from $14.3 billion in 1980, to 2080 estimates of $14.1 billion for the RCP4.5 climate scenario (a 1% decrease) and $14.5 billion for the RCP 8.5 climate scenario (a 1% increase).

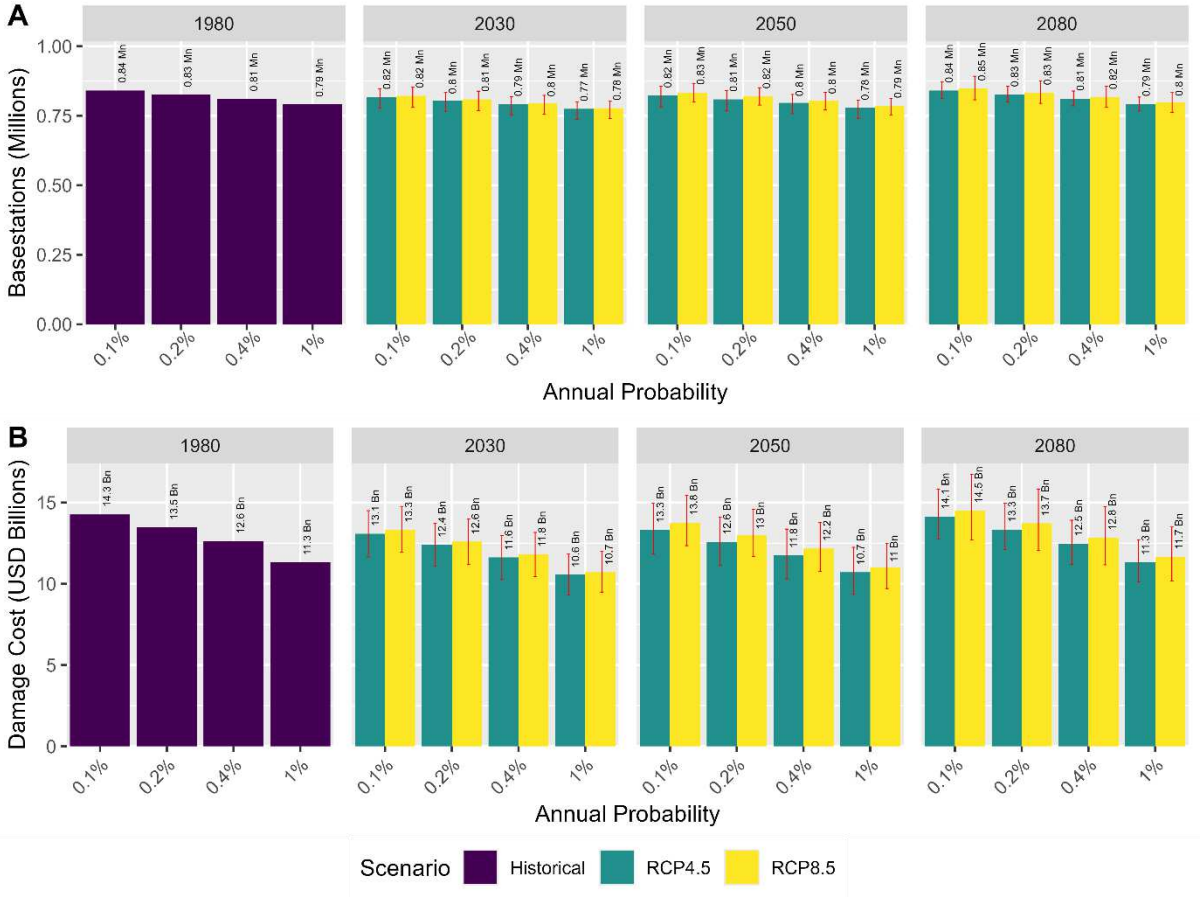


Figure 5 (A) Estimated riverine flooding impact to mobile voice/data basestations, reported by annual probability, year and climate scenario, (B) Estimated riverine flooding direct cost impact, reported by annual probability, year and climate scenario.

Riverine impacts are visualized in Figure 6 for the RCP8.5 scenario in 2080, with an annual probability of 0.01% (1-in-1000-year). Subplot (A) illustrates the cost density (adjusting for statistical area size), and subplot (B) visualizes the total cost per statistical area. The estimated damage values represent the mean average across the model variants. Large damage impacts are estimated for Eastern Europe (e.g., Germany, Poland etc.), Latin America (e.g., Brazil), southeast Asia (e.g., Indonesia), east Asia (e.g., Japan and Korea), and central Asia (e.g., Russia and Kazakhstan).

Again, the largest impacts are present in high income countries (approximately 60%), followed by 29% in UMCs, 11% in LMCs and <1% in LICs. Compared to coastal flooding, the level of vulnerability to riverine flooding is more evenly spread across regions. For example, Asia comprises approximately 42% of the impacts, followed by 29% in Europe, 20% in North America, 4% in South America, and roughly 3% each in Africa and Oceania.

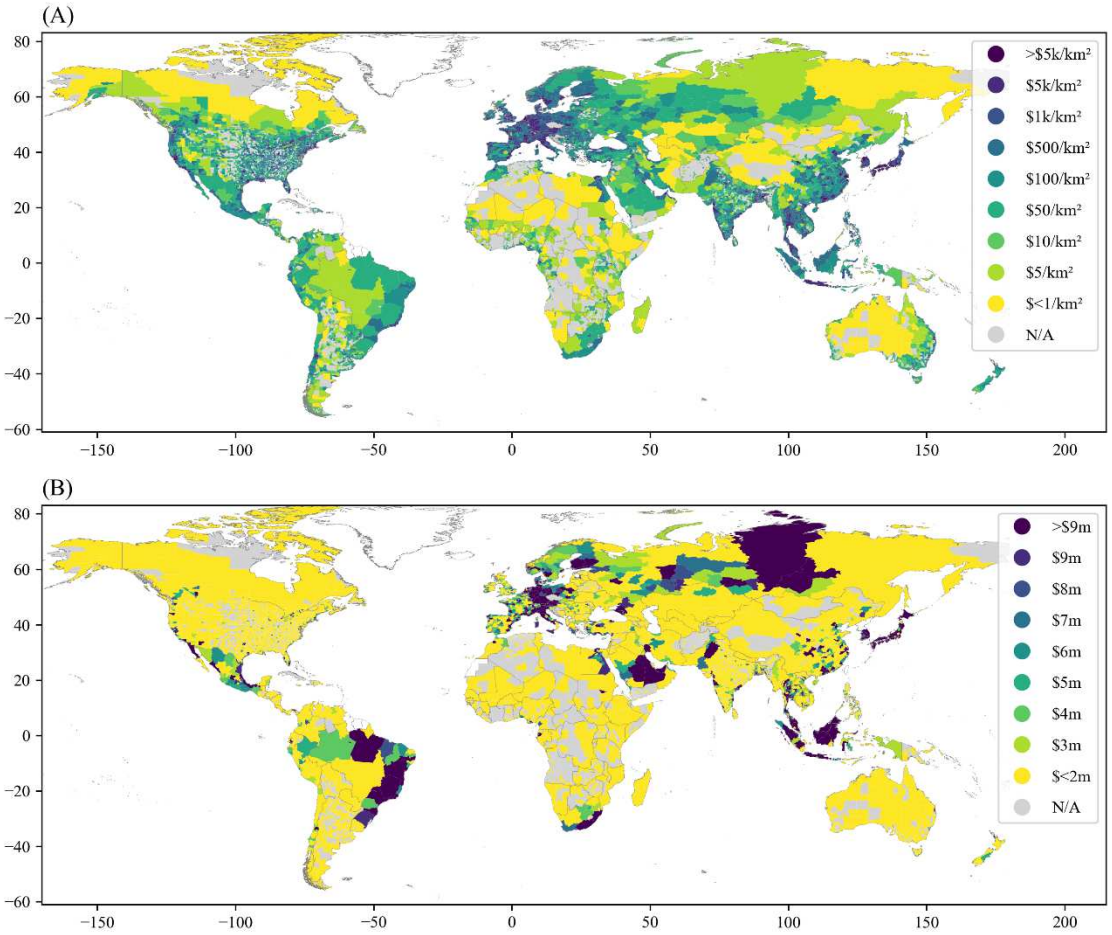


Figure 6 (A) Cost density of estimated riverine flooding direct damage ($/km2), (B) Total cost of estimated riverine flooding direct damage ($ millions).

4.3. Vulnerability to tropical cyclones

Figure 7 (A) illustrates the mobile base station vulnerability results for tropical cyclone hazards, for different years and annual probabilities of occurrence. Two scenarios exist, including a 1980 historical climate scenario, and then a future 2050 climate scenario equivalent to RCP8.5. Approximately 0.51 million base stations are estimated to be affected in the 1980 historical baseline for an event with a 1% annual probability, rising to 0.97 million in 2050 for an RCP8.5 scenario (an increase of 90%). This compares to 1.34 million base stations in the 1980 historical baseline for an event with a 0.01% annual probability, increasing to 1.61 million by 2050 for the RCP8.5 scenario (an increase of 20%).

The direct damage cost is also illustrated for a set of historical scenarios, as reported in Figure 7 (B). The results indicate very large differences in vulnerability. For example, for the smallest event size, with a 1% annual probability (a 1-in-100-year return period), the total direct economic damage is estimated at $1.16 billion for the 1980 historical scenario, with 41% of this impact in Europe, 24% in North America and 20% in Asia. In contrast, under the more severe 2050 climate scenario, the estimated damage reaches $1.28 billion (an increase of 10%), with 33% of this impact in Europe, 26% in North America and 22% in Asia. In contrast, in the second-to-largest event size with a 0.1% annual occurrence (a return period of 1-in-1000-years), the historical vulnerability is estimated at $1.46 billion, with 37% of this impact in Europe, 23% in North America and 22% in Asia. This is compared to the future 2050 climate scenario estimate of $1.62 billion (an 11% increase), where approximately 35% of the damage is in Europe, 25% in North America, 21% in Asia, and 15% in Oceania.

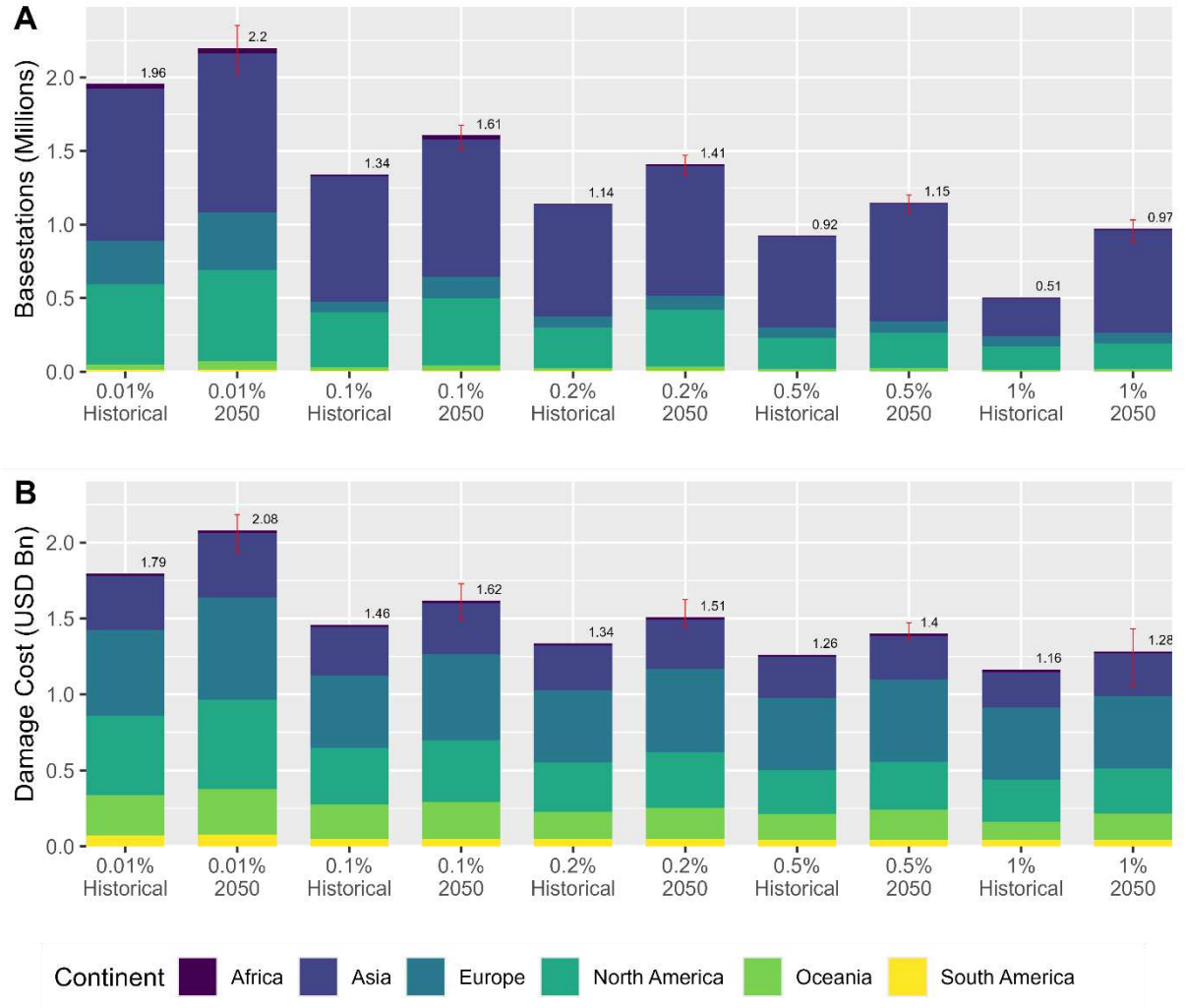


Figure 7 (A) Estimated tropical cyclone impact to mobile voice/data basestations, reported by annual probability, year and climate scenario, (B) Estimated tropical cyclone direct cost impact, reported by annual probability, year and climate scenario.

In Figure 8 the estimated mean damage cost is visualized globally for an event with a 0.01% annual probability (1-in-1000-year), for the latest time point available (2050), in an RCP8.5 scenario. Firstly, subplot (A) illustrates the cost density (adjusting for statistical area size), and subplot (B) visualizes the total cost per statistical area. The largest damage impacts are visible in East Asia (e.g., Japan, South Korea and China), South Asia (e.g., India, Pakistan and Bangladesh), Western Europe (e.g., UK and France), North Africa (e.g., Morocco), and in North and Central America (e.g., the USA, Mexico, Panama, Colombia). While Japan and South Korea indicate high levels of potential damage nationally, in the Americas, key vulnerable regions include Florida in the USA, and Yucatan and Tamaulipas in Mexico. Equally, the Andalucía region of southern Spain (containing Seville) sees elevate vulnerability, along with the Sindh area of Pakistan (containing Karachi).

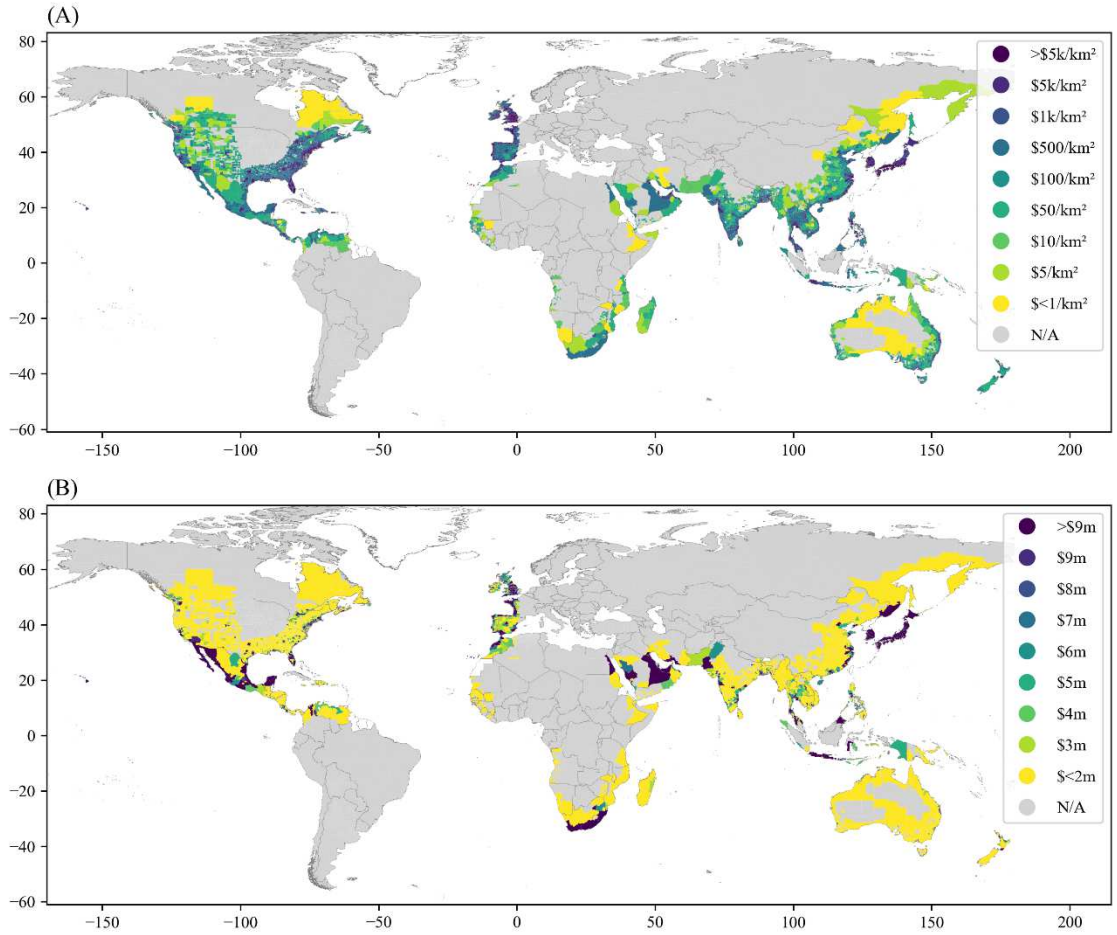


Figure 8 (A) Density of estimated tropical cyclone flooding damage cost ($/km^2), (B) Total estimated tropical cyclone damage cost ($ millions)

5. Discussion

For the 6 million cellular assets assessed for 2G, 3G, 4G and 5G, the results vary strongly for countries, income groups and regions. These estimates reflect both the spatial hazard differences across countries, and the spatial distribution of the base stations present in the underlying data.

How many cellular assets are potentially vulnerable to climate hazards, such as coastal flooding, riverine flooding, and tropical cyclones?

For coastal flooding, the quantity of cells vulnerable from an event with a 1% annual probability is estimated at 42.5 thousand for the historical 1980 climate scenario, increasing by 2080 to 67.7 thousand for RCP4.5 (a 59% increase) and 74.4 thousand for RCP8.5 (a 75% increase). Moreover, an event with a 0.1% annual probability in the 1980 historical climate baseline is estimated to affect 52.6 thousand base stations, versus 83 thousand in the RCP4.5 scenario (a 56% increase), and 92.2 thousand base stations in the RCP8.5 climate scenario (a 75% increase).

For riverine flooding, estimates suggest that for a 1980 historical baseline the total number of vulnerable base stations for an event with a 1% annual probability is 0.79 million. Under the RCP4.5 scenario this remains static at 0.79 million, whereas there is a marginal increase for the RCP8.5 scenario to 0.8 million vulnerable base stations (a 1% increase). For events with a 0.1% annual probability, approximately 0.84 million base stations are at risk for the 1980 historical baseline, remaining static at 0.84 million base stations in the RCP4.5 scenario in 2080, and increasing to 0.85 million base stations in the RCP4.5 scenario (a 1% increase).

The estimates reached for tropical cyclones suggest many base stations could be affected. For example, for an event with a 1% annual probability, 0.51 million affected base stations are estimated as experiencing some form of damage, with this increasing by 2050 in an RCP8.5 scenario to 0.97 million (a 90% increase). For a much larger event with a 0.1% annual probability, the 1980 historical baseline sees 1.34 million base stations potentially affected, increasing by 2050 for the RCP8.5 scenario to 1.61 million (a 20% increase).

What magnitude of direct economic damage may occur from different climate hazard scenarios, for example from coastal flooding, riverine flooding, and tropical cyclones?

The direct economic damage estimates for coastal flooding range from $0.95 billion an event with a 1% annual probability in the 1980 historical baseline, up to $1.56 billion by 2080 in the RCP4.5 scenario, or $1.76 billion in the RCP8.5 scenario (an increase of 64% and 85%, respectively). Compared to a more extreme scenario with a 0.1% annual probability, a $1.22 billion estimate is produced for the 1980 historical baseline, rising to $2 billion in the RCP4.5 scenario (an increase of 64%), and 2.26 billion in the RCP8.5 scenario (an increase of 85%) by 2080.

Riverine flooding produced a different trend, as the less severe case with a 1% annual probability had a direct damage estimate of $11.3 billion in the historical 1980 baseline, compared to $11.3 billion in

the RCP4.5 climate scenario (a 1% decrease), and $11.7 billion in the RCP8.5 climate scenario in 2080 (a 4% increase). In the more severe event case of 0.1% annual probability (a 1-in-1000-year return period), the direct damage estimate ranges from $14.3 billion in the 1980 historical baseline, to $14.1 billion for the RCP4.5 climate scenario (a 1% decrease) and $14.5 billion for the RCP 8.5 climate scenario in 2080 (a 1% increase).

Finally, for tropical cyclone event sizes with a 1% annual probability the direct damage estimate ranges from $1.16 billion in the 1980 historical baseline, to $1.28 billion in 2050 under an RCP8.5 scenario, increasing by 10%. For a much larger event with a 0.1% annual occurrence, the direct damage estimate for the 1980 historical baseline is $1.46 billion, rising significantly to $1.62 billion for a future 2050 climate scenario, increasing by 11%.

6. Conclusions

In this paper a global assessment was undertaken evaluating the potential impacts to mobile cellular infrastructure for a variety of climate scenarios. Using open crowdsourced data equating to 6 million 2G, 3G, 4G and 5G unique base stations, a variety of climate scenarios were explored, quantifying potentially damaged assets and direct damage costs. The results were reported for a range of event sizes with different annual probabilities. The paper contributes to the literature one of the first global assessments of mobile cellular infrastructure for climate related hazards.

In the baseline historical scenarios for an event with a 0.1% annual probability, the largest number of affected base stations was found to be from tropical cyclones (1.34 m), followed by riverine flooding (0.84 m) and coastal flooding (52.6 thousand). However, the number of affected base stations did not necessarily yield the same magnitude in terms of direct damage impacts. For example, the historical estimated damage cost was $1.46 billion for tropical cyclones, $14.3 billion riverine flooding, followed by $1.22 billion for coastal flooding. The results suggest that many base stations can be affected by high winds from tropical cyclones but may only receive very minor damage.

When examining the impacts under future climate scenarios, the results suggest that tropical cyclones and coastal flooding see the largest increases in the most severe high emissions futures explored. For example, for a 0.1% annual probability event under RCP8.5, the number of affected base stations is estimated to rise to 1.61 million for tropical cyclones (an increase of 20%), equating to $1.62 billion in direct damage (an increase of 11%). Equally, for coastal flooding the number of potentially affected base stations for an event with a 0.1% annual probability under RCP8.5 is 92.2 thousand (an increase of 75%), equating to direct damage costs of $2.26 billion (an increase of 85%). Riverine flooding saw estimates remain relatively static, due to many mountainous areas having lower winter snowfall, and therefore smaller meltwater runoff leading to flooding events.

The findings demonstrate the need for risk analysts to include mobile communications (and telecommunications more broadly) in future critical infrastructure assessments. Indeed, this paper contributes a proven assessment methodology to the literature for use in future research for assessing this critical infrastructure sector.

Acknowledgements

This research endeavor has been supported by funding from multiple sources. These include the World Bank Digital Development Global Practice (as background evidence for the report Catalyzing the Green Digital Transformation in Low- and Middle-Income Economies, and Climate Change Development Reports for Azerbaijan, Kenya, and the Democratic Republic of Congo), and the Insurance Development Forum (as part of the Global Resilience Index Initiative).

References

Argyroudis, S.A., Mitoulis, S.A., Chatzi, E., Baker, J.W., Brilakis, I., Gkoumas, K., Vousdoukas, M., Hynes, W., Carluccio, S., Keou, O., Frangopol, D.M., Linkov, I., 2022. Digital technologies can enhance climate resilience of critical infrastructure. Climate Risk Management 35, 100387. https://doi.org/10.1016/j.crm.2021.100387

Bauer, J.M., Bohlin, E., 2022. Regulation and innovation in 5G markets. Telecommunications Policy, Innovation in 5G technology: leadership, competition and policy issues. 46, 102260. https://doi.org/10.1016/j.telpol.2021.102260

Bello, O., Williams, R., Hendrickson, M., De Andrade, R., Mery, G., Bazo, A., De Quattro, J., Ibarra, F., Marcano, B., Marconi, S., 2020. Assessment of the Effects and Impacts of Hurricane Matthew, The Bahamas. Inter-American Development Bank, Washington D.C.

Bernhofen, M.V., Whyman, C., Trigg, M.A., Sleigh, P.A., Smith, A.M., Sampson, C.C., Yamazaki, D., Ward, P.J., Rudari, R., Pappenberger, F., Dottori, F., Salamon, P., Winsemius, H.C., 2018. A first collective validation of global fluvial flood models for major floods in Nigeria and Mozambique. Environ. Res. Lett. 13, 104007. https://doi.org/10.1088/1748-9326/aae014

Bloemendaal, N., De Moel, H., Muis, S., Haigh, I.D., Aerts, J., 2022. STORM tropical cyclone wind speed return periods. https://doi.org/10.4121/12705164.v3

Bloemendaal, N., Haigh, I.D., de Moel, H., Muis, S., Haarsma, R.J., Aerts, J.C.J.H., 2020. Generation of a global synthetic tropical cyclone hazard dataset using STORM. Sci Data 7, 40. https://doi.org/10.1038/s41597-020-0381-2

Blöschl, G., Hall, J., Viglione, A., Perdigão, R.A.P., Parajka, J., Merz, B., Lun, D., Arheimer, B., Aronica, G.T., Bilibashi, A., Boháč, M., Bonacci, O., Borga, M., Čanjevac, I., Castellarin, A., Chirico, G.B., Claps, P., Frolova, N., Ganora, D., Gorbachova, L., Gül, A., Hannaford, J., Harrigan, S., Kireeva, M., Kiss, A., Kjeldsen, T.R., Kohnová, S., Koskela, J.J., Ledvinka, O., Macdonald, N., Mavrova-Guirguinova, M., Mediero, L., Merz, R., Molnar, P., Montanari, A., Murphy, C., Osuch, M., Ovcharuk, V., Radevski, I., Salinas, J.L., Sauquet, E., Šraj, M., Szolgay, J., Volpi, E., Wilson, D., Zaimi, K., Živković, N., 2019. Changing climate both increases and decreases European river floods. Nature 573, 108–111. https://doi.org/10.1038/s41586-019-1495-6

Booker, G., Torres, J., Guikema, S., Sprintson, A., Brumbelow, K., 2010. Estimating cellular network performance during hurricanes. Reliability Engineering & System Safety 95, 337–344. https://doi.org/10.1016/j.ress.2009.11.003

Brewer, E., Lin, J., Kemper, P., Hennin, J., Runfola, D., 2021. Predicting road quality using high resolution satellite imagery: A transfer learning approach. PLOS ONE 16, e0253370. https://doi.org/10.1371/journal.pone.0253370

Broberg, M., 2020. Parametric loss and damage insurance schemes as a means to enhance climate change resilience in developing countries. Climate Policy 20, 693–703. https://doi.org/10.1080/14693062.2019.1641461

Carter, L., Milliman, J.D., Talling, P.J., Gavey, R., Wynn, R.B., 2012. Near-synchronous and delayed initiation of long run-out submarine sediment flows from a record-breaking river flood, offshore Taiwan. Geophysical Research Letters 39. https://doi.org/10.1029/2012GL051172

Cave, M., 2018. How disruptive is 5G? Telecommunications Policy, The implications of 5G networks: Paving the way for mobile innovation? 42, 653–658. https://doi.org/10.1016/j.telpol.2018.05.005

Coughlan de Perez, E., Harrison, L., Berse, K., Easton-Calabria, E., Marunye, J., Marake, M., Murshed, S.B., Shampa, Zauisomue, E.-H., 2022. Adapting to climate change through anticipatory action: The potential use of weather-based early warnings. Weather and Climate Extremes 38, 100508. https://doi.org/10.1016/j.wace.2022.100508

da Ponte, A., Leon, G., Alvarez, I., 2023. Technological sovereignty of the EU in advanced 5G mobile communications: An empirical approach. Telecommunications Policy 47, 102459. https://doi.org/10.1016/j.telpol.2022.102459

Dallimer, M., Martin-Ortega, J., Rendon, O., Afionis, S., Bark, R., Gordon, I.J., Paavola, J., 2020. Taking stock of the empirical evidence on the insurance value of ecosystems. Ecological Economics 167, 106451. https://doi.org/10.1016/j.ecolecon.2019.106451

DHS, FEMA, 2011. Hazus-MH MR3 flood technical manual. Version 2.1. Flood Model.
Dottori, F., Szewczyk, W., Ciscar, J.-C., Zhao, F., Alfieri, L., Hirabayashi, Y., Bianchi, A., Mongelli, I., Frieler, K., Betts, R.A., Feyen, L., 2018. Increased human and economic losses from river flooding with anthropogenic warming. Nature Clim Change 8, 781–786. https://doi.org/10.1038/s41558-018-0257-z
Eiselt, H.A., Marianov, V., 2012. Mobile phone tower location for survival after natural disasters. European Journal of Operational Research 216, 563–572. https://doi.org/10.1016/j.ejor.2011.08.021
EL Khaled, Z., Mcheick, H., 2019. Case studies of communications systems during harsh environments: A review of approaches, weaknesses, and limitations to improve quality of service. International Journal of Distributed Sensor Networks 15, 1550147719829960. https://doi.org/10.1177/1550147719829960
El-Bawab, T.S., 2021. Network Engineering versus Climate Change. IEEE Communications Magazine 59, 6–7. https://doi.org/10.1109/MCOM.2021.9422338
Federal Communications Commission, 2017. Communications Status Report for Areas Impacted by Tropical Storm Harvey August 27, 2017. Federal Communications Commission (FCC), Washington D.C.
Federal Communications Commission, 2006. Independent Panel Reviewing the Impact of Hurricane Katrina on Communications Networks. Report and Recommendations for the Federal Communications Commission. Federal Communications Commission (FCC), Washington D.C.
Foster, C., 2011. Earthquake performance of telecommunications infrastructure in Christchurch 2010 / 2011, in: 2011 IEEE 33rd International Telecommunications Energy Conference (INTELEC). Presented at the 2011 IEEE 33rd International Telecommunications Energy Conference (INTELEC), pp. 1–5. https://doi.org/10.1109/INTLEC.2011.6099735
Gallarno, G., Muniz, J., Parnell, G.S., Pohl, E.A., Wu, J., 2023. Development and assessment of a resilient telecoms system. Journal of Defense Modeling & Simulation 15485129221143791. https://doi.org/10.1177/15485129221143791
Gössling, S., Neger, C., Steiger, R., Bell, R., 2023. Weather, climate change, and transport: a review. Nat Hazards 118, 1341–1360. https://doi.org/10.1007/s11069-023-06054-2
Hall, J.W., Thacker, S., Ives, M.C., Cao, Y., Chaudry, M., Blainey, S.P., Oughton, E.J., 2017. Strategic analysis of the future of national infrastructure. Proceedings of the Institution of Civil Engineers - Civil Engineering 170, 39–47. https://doi.org/10.1680/jcien.16.00018
Hall, J.W., Tran, M., Hickford, A.J., Nicholls, R.J., 2016. The future of national infrastructure: A system-of-systems approach. Cambridge University Press.
Hallegatte, S., Rozenberg, J., Rentschler, J., Nicolas, C., Fox, C., 2019. Strengthening New Infrastructure Assets: A Cost-Benefit Analysis, Policy Research Working Papers. The World Bank. https://doi.org/10.1596/1813-9450-8896
Hermans, T.D.G., Šakić Trogrlić, R., van den Homberg, M.J.C., Bailon, H., Sarku, R., Mosurska, A., 2022. Exploring the integration of local and scientific knowledge in early warning systems for disaster risk reduction: a review. Nat Hazards 114, 1125–1152. https://doi.org/10.1007/s11069-022-05468-8
Hoßfeld, T., Varela, M., Skorin-Kapov, L., Heegaard, P.E., 2023. A Greener Experience: Trade-Offs between QoE and CO2 Emissions in Today's and 6G Networks. IEEE Communications Magazine 61, 178–184. https://doi.org/10.1109/MCOM.006.2200490
Jakubek, R.R., 2015. Nonequivalent Quasi-Experimental Study of Wireless Telecommunication Traffic During Severe Winter Storms. IEEE Access 3, 1036–1041. https://doi.org/10.1109/ACCESS.2015.2450675
Kaja, H., Paropkari, R.A., Beard, C., Van De Liefvoort, A., 2021. Survivability and Disaster Recovery Modeling of Cellular Networks Using Matrix Exponential Distributions. IEEE Transactions on Network and Service Management 18, 2812–2824. https://doi.org/10.1109/TNSM.2021.3090355
Kok, M., Huizinga, H.J., Vrouwenvelder, A.C.W.M., Barendregt, A., 2005. Standard method 2004 damage and casualties caused by flooding - Rijkswaterstaat Rapportendatabank (No. DWW-2005-009).

Koks, E.E., Le Bars, D., Essenfelder, A.H., Nirandjan, S., Sayers, P., 2022. The impacts of coastal flooding and sea level rise on critical infrastructure: a novel storyline approach. Sustainable and Resilient Infrastructure 0, 1–25. https://doi.org/10.1080/23789689.2022.2142741

Koks, E.E., Rozenberg, J., Zorn, C., Tariverdi, M., Vousdoukas, M., Fraser, S.A., Hall, J.W., Hallegatte, S., 2019. A global multi-hazard risk analysis of road and railway infrastructure assets. Nature Communications 10, 2677. https://doi.org/10.1038/s41467-019-10442-3

Krishnamurthy, V., Kwasinski, A., Dueñas-Osorio, L., 2016. Comparison of Power and Telecommunications Dependencies and Interdependencies in the 2011 Tohoku and 2010 Maule Earthquakes. Journal of Infrastructure Systems 22, 04016013. https://doi.org/10.1061/(ASCE)IS.1943-555X.0000296

Kwasinski, A., 2013. Effects of Hurricanes Isaac and Sandy on Data and Communications Power Infrastructure, in: Intelec 2013; 35th International Telecommunications Energy Conference, SMART POWER AND EFFICIENCY. Presented at the Intelec 2013; 35th International Telecommunications Energy Conference, SMART POWER AND EFFICIENCY, pp. 1–6.

Kwasinski, A., 2011. Effects of notable natural disasters from 2005 to 2011 on telecommunications infrastructure: Lessons from on-site damage assessments, in: 2011 IEEE 33rd International Telecommunications Energy Conference (INTELEC). Presented at the 2011 IEEE 33rd International Telecommunications Energy Conference (INTELEC), pp. 1–9. https://doi.org/10.1109/INTLEC.2011.6099777

Kwasinski, A., Weaver, W.W., Chapman, P.L., Krein, P.T., 2009. Telecommunications Power Plant Damage Assessment for Hurricane Katrina– Site Survey and Follow-Up Results. IEEE Systems Journal 3, 277–287. https://doi.org/10.1109/JSYST.2009.2026783

Kwon, Y., Kwasinski, Alexis, Kwasinski, Andres, 2016. Coordinated Energy Management in Resilient Microgrids for Wireless Communication Networks. IEEE Journal of Emerging and Selected Topics in Power Electronics 4, 1158–1173. https://doi.org/10.1109/JESTPE.2016.2614425

Lehr, W., Queder, F., Haucap, J., 2021. 5G: A new future for Mobile Network Operators, or not? Telecommunications Policy 45, 102086. https://doi.org/10.1016/j.telpol.2020.102086

Marshall, A., Wilson, C.-A., Dale, A., 2023. Telecommunications and natural disasters in rural Australia: The role of digital capability in building disaster resilience. Journal of Rural Studies 100, 102996. https://doi.org/10.1016/j.jrurstud.2023.03.004

Miyamoto International, World Bank, 2019. Overview of engineering options for increasing infrastructure resilience. World Bank, Washington D.C.

Mohebbi, S., Zhang, Q., Christian Wells, E., Zhao, T., Nguyen, H., Li, M., Abdel-Mottaleb, N., Uddin, S., Lu, Q., Wakhungu, M.J., Wu, Z., Zhang, Y., Tuladhar, A., Ou, X., 2020. Cyber-physical-social interdependencies and organizational resilience: A review of water, transportation, and cyber infrastructure systems and processes. Sustainable Cities and Society 62, 102327. https://doi.org/10.1016/j.scs.2020.102327

Movahednia, M., Kargarian, A., Ozdemir, C.E., Hagen, S.C., 2022. Power Grid Resilience Enhancement via Protecting Electrical Substations Against Flood Hazards: A Stochastic Framework. IEEE Transactions on Industrial Informatics 18, 2132–2143. https://doi.org/10.1109/TII.2021.3100079

Nirandjan, S., Koks, E.E., Ward, P.J., Aerts, J.C.J.H., 2022. A spatially-explicit harmonized global dataset of critical infrastructure. Sci Data 9, 150. https://doi.org/10.1038/s41597-022-01218-4

O'Reilly, G., Jrad, A., Nagarajan, R., Brown, T., Conrad, S., 2006. Critical Infrastructure Analysis of Telecom for Natural Disasters, in: Networks 2006. 12th International Telecommunications Network Strategy and Planning Symposium. Presented at the Networks 2006. 12th International Telecommunications Network Strategy and Planning Symposium, pp. 1–6. https://doi.org/10.1109/NETWKS.2006.300396

Othman, A., Kaddoum, G., C. Evangelista, J.V., Au, M., Agba, B.L., 2023. Digital Twinning in Smart Grid Networks: Interplay, Resource Allocation and Use Cases. IEEE Communications Magazine 61, 120–126. https://doi.org/10.1109/MCOM.001.2200823

Oughton, E.J., Boch, E., Kusuma, J., 2022a. Engineering-Economic Evaluation of Diffractive NLOS Backhaul (e3nb): A Techno-economic Model for 3D Wireless Backhaul Assessment. IEEE Access 10, 3430–3446. https://doi.org/10.1109/ACCESS.2022.3140421

Oughton, E.J., Comini, N., Foster, V., Hall, J.W., 2022b. Policy choices can help keep 4G and 5G universal broadband affordable. Technological Forecasting and Social Change 176, 121409. https://doi.org/10.1016/j.techfore.2021.121409

Oughton, E.J., Frias, Z., Dohler, M., Whalley, J., Sicker, D., Hall, J.W., Crowcroft, J., Cleevely, D.D., 2018. The strategic national infrastructure assessment of digital communications. Digital Policy, Regulation and Governance.

Oughton, E.J., Lehr, W., 2022. Surveying 5G Techno-Economic Research to Inform the Evaluation of 6G Wireless Technologies. IEEE Access 10, 25237–25257. https://doi.org/10.1109/ACCESS.2022.3153046

Oughton, E.J., Lehr, W., Katsaros, K., Selinis, I., Bubley, D., Kusuma, J., 2021. Revisiting Wireless Internet Connectivity: 5G vs Wi-Fi 6. Telecommunications Policy 45, 102127. https://doi.org/10.1016/j.telpol.2021.102127

Oughton, E.J., Mathur, J., 2021. Predicting cell phone adoption metrics using machine learning and satellite imagery. Telematics and Informatics 62, 101622. https://doi.org/10.1016/j.tele.2021.101622

Pant, R., Russell, T., Zorn, C., Oughton, E., Hall, J.W., 2020. Resilience study research for NIC–systems analysis of interdependent network vulnerabilities. Environmental Change Institute.

Pörtner, H.O., Roberts, D.C., Adams, H., Adler, C., Aldunce, P., Ali, E., Begum, R.A., Betts, R., Kerr, R.B., Biesbroek, R., Birkmann, J., Bowen, K., Castellanos, E., Cissé, G., Constable, A., Cramer, W., Dodman, D., Eriksen, S.H., Fischlin, A., Garschagen, M., Glavovic, B., Gilmore, E., Haasnoot, M., Harper, S., Hasegawa, T., Hayward, B., Hirabayashi, Y., Howden, M., Kalaba, K., Kiessling, W., Lasco, R., Lawrence, J., Lemos, M.F., Lempert, R., Ley, D., Lissner, T., Lluch-Cota, S., Loeschke, S., Lucatello, S., Luo, Y., Mackey, B., Maharaj, S., Mendez, C., Mintenbeck, K., Vale, M.M., Morecroft, M.D., Mukherji, A., Mycoo, M., Mustonen, T., Nalau, J., Okem, A., Ometto, J.P., Parmesan, C., Pelling, M., Pinho, P., Poloczanska, E., Racault, M.-F., Reckien, D., Pereira, J., Revi, A., Rose, S., Sanchez-Rodriguez, R., Schipper, E.L.F., Schmidt, D., Schoeman, D., Shaw, R., Singh, C., Solecki, W., Stringer, L., Thomas, A., Totin, E., Trisos, C., Viner, D., Aalst, M. van, Wairiu, M., Warren, R., Yanda, P., Ibrahim, Z.Z., 2022. Climate change 2022: impacts, adaptation and vulnerability.

Pourghasemi, H.R., Gayen, A., Edalat, M., Zarafshar, M., Tiefenbacher, J.P., 2020. Is multi-hazard mapping effective in assessing natural hazards and integrated watershed management? Geoscience Frontiers 11, 1203–1217. https://doi.org/10.1016/j.gsf.2019.10.008

Roberts, M.J., Camp, J., Seddon, J., Vidale, P.L., Hodges, K., Vanniere, B., Mecking, J., Haarsma, R., Bellucci, A., Scoccimarro, E., Caron, L.-P., Chauvin, F., Terray, L., Valcke, S., Moine, M.-P., Putrasahan, D., Roberts, C., Senan, R., Zarzycki, C., Ullrich, P., 2020. Impact of Model Resolution on Tropical Cyclone Simulation Using the HighResMIP–PRIMAVERA Multimodel Ensemble. Journal of Climate 33, 2557–2583. https://doi.org/10.1175/JCLI-D-19-0639.1

Rosario-Albert, L., Takahashi, B., 2021. Emergency communications policies in Puerto Rico: Interaction between regulatory institutions and telecommunications companies during Hurricane Maria. Telecommunications Policy 45, 102094. https://doi.org/10.1016/j.telpol.2020.102094

Russell, T., 2022. STORM tropical cyclone wind speed return periods as global GeoTIFFs. https://doi.org/10.5281/zenodo.7438145

Sánchez-Muñoz, D., Domínguez-García, J.L., Martínez-Gomariz, E., Russo, B., Stevens, J., Pardo, M., 2020. Electrical Grid Risk Assessment Against Flooding in Barcelona and Bristol Cities. Sustainability 12, 1527. https://doi.org/10.3390/su12041527

Simpson, N.P., Mach, K.J., Constable, A., Hess, J., Hogarth, R., Howden, M., Lawrence, J., Lempert, R.J., Muccione, V., Mackey, B., New, M.G., O'Neill, B., Otto, F., Pörtner, H.-O., Reisinger, A., Roberts, D., Schmidt, D.N., Seneviratne, S., Strongin, S., Aalst, M. van, Totin, E., Trisos, C.H., 2021. A framework for complex climate change risk assessment. One Earth 4, 489–501. https://doi.org/10.1016/j.oneear.2021.03.005

Suryakumar, V.S., Liu, Z., Thomsen, B., Tiwari, A., Varkey, P., Marriott, J., 2020. Aeroelastic Preliminary-Design Optimization of Communication Tower Structures, in: AIAA Scitech

2020 Forum. American Institute of Aeronautics and Astronautics. https://doi.org/10.2514/6.2020-1634

van Vliet, M.T.H., Wiberg, D., Leduc, S., Riahi, K., 2016. Power-generation system vulnerability and adaptation to changes in climate and water resources. Nature Clim Change 6, 375–380. https://doi.org/10.1038/nclimate2903

Verschuur, J., Fernández-Pérez, A., Mühlhofer, E., Nirandjan, S., Borgomeo, E., Becher, O., Voskaki, A., Oughton, E.J., Stankovski, A., Greco, S.F., Koks, E.E., Pant, R., Hall, J.W., 2024. Quantifying climate risks to infrastructure systems: A comparative review of developments across infrastructure sectors. PLOS Climate 3, e0000331. https://doi.org/10.1371/journal.pclm.0000331

Verschuur, J., Koks, E.E., Hall, J.W., 2023. Systemic risks from climate-related disruptions at ports. Nat. Clim. Chang. 13, 804–806. https://doi.org/10.1038/s41558-023-01754-w

Woetzel, J., Pinner, D., Samandari, H., 2020. Climate risk and response: Physical hazards and socioeconomic impacts. Will mortgages and markets stay afloat in Florida? McKinsey Global Institute, New York, NY.

World Resources Institute, 2022. Aqueduct Floods Hazard Maps [WWW Document]. World Resources Institute. URL https://www.wri.org/data/aqueduct-floods-hazard-maps (accessed 2.24.22).

Wuebbles, D.J., Fahey, D.W., Hibbard, K.A., Arnold, J.R., DeAngelo, B., Doherty, S., Easterling, D.R., Edmonds, J., Edmonds, T., Hall, T., Hayhoe, K., Huffman, F.M., Horton, R., Huntzinger, D., Jewett, L., Knutson, T., Kopp, R.E., Kossin, J.P., Kunkel, K.E., LeGrande, A.N., Leung, L.R., Maslowski, W., Mears, C., Perlwitz, J., Romanou, A., Sanderson, B.M., Sweet, W.V., Taoylor, P.C., Trapp, R.J., Vose, R.S., Waliser, D.E., Wehner, M.F., West, T.O., Alley, R., Armstrong, C.T., Bruno, J., Busch, S., Champion, S., Durre, I., Gledhill, D., Goldstein, J., Huang, B., Krishnan, H., Levin, L., Muller-Karger, F., Rhoades, A., Stevens, L., Sun, L., Takle, E., Ullrich, P., Wahl, E., Walsh, J., 2017. Climate Science Special Report: Fourth National Climate Assessment (NCA4), Volume I (Report). USGCRP.

Yousefi, S., Pourghasemi, H.R., Emami, S.N., Pouyan, S., Eskandari, S., Tiefenbacher, J.P., 2020. A machine learning framework for multi-hazards modeling and mapping in a mountainous area. Sci Rep 10, 12144. https://doi.org/10.1038/s41598-020-69233-2

Supplementary information

S1 Hazard scenario metrics

In S1 (A) the mean inundation depth is presented for coastal flooding, for four different annual probabilities, disaggregated by continent. Generally, the historical mean depth for 1980 is lower than the forecast years, across the two climate scenarios. For example, for a 1-in-100-year event size with a 1% annual probability, the 1980 mean depth is 4.58 m based across all flooded 1 km^2 tiles. In contrast, this value increases to 5.44 m by 2080 for the RCP4.5 scenario, or 5.66 m in the RCP8.5 scenario, again for the final year of the assessment period. In contrast, a larger event equating to a 1-in-1000-year return period, with a 0.1% annual probability, the historical mean depth is 4.77 m, increasing by 2080 to 5.87 m in RCP4.5, and 6.09 m in RCP8.5. The hazard dynamics illustrated are consistent with *a priori* expectations for how climate change will affect coastal flooding.



S1 Hazard variance by scenario

In S1 (B) the results are presented for riverine flooding by continent, focusing on the mean inundation depth for all flooded 1 km^2 tiles. In the 1980 historical baseline, for riverine flooding events with a 1% annual probability (1-in-100-year return period), a mean value of 4.23 m is obtained, and contrasts with 4.11 m in 2080 in the RCP4.5 scenario, and 4.5 m in the RCP8.5 scenario. These mean averages are

logically higher for larger events with lower annual probabilities, such as a 1-in-1000-year magnitude (0.01% annual probability). For example, in the 1980 historical baseline the mean inundation depth is 6.32 m, rising to 5.76 m in the RCP4.5 scenario, and 6.36 m in the RCP8.5 scenario.

Whereas in the coastal mean averages, there is a clear relationship from a more severe climate scenario leading to increased flooding, this is not so clearly pronounced for riverine flooding. Yet, this is consistent with other studies in the literature which have demonstrated that some regions may see increased flooding, while others may see decreasing flooding levels. For example, a warmer climate may lead to lower winter snow levels in mountainous areas, consequently producing smaller meltwater volumes in spring and summer months in many catchment areas. Thus, the mean average inundation depth may be static or declining in such circumstances.